

Scanning-tunneling-microscopy and spectroscopy simulation of the GaAs(110) surface

J. M. Bass and C. C. Matthai

Department of Physics and Astronomy, University of Wales College of Cardiff, P.O. Box 913, Cardiff CF2 3YB, Wales, United Kingdom

(Received 7 March 1995)

We have generated, using an *ab initio* pseudopotential method and the Bardeen transfer Hamiltonian approximation, scanning-tunneling-microscopy images and scanning-tunneling-spectroscopy spectra of the GaAs(110) surface. The surface was fully relaxed and a cluster of four Al atoms was used to represent the tip. We investigate the effect of different tip-surface bias voltages on the scanning-tunneling microscopy images and compare them to experimental results. In particular, the effectiveness of using the images to determine the buckling angle of the surface bond is discussed. For the scanning-tunneling-spectroscopy spectra, different lateral tip positions were utilized and various features associated with surface states were identified, which we also compare with experiment.

There are a number of different operating modes for the scanning tunneling microscope (STM). The most obvious is to use the STM to image a solid surface to obtain information concerning the atomic structure of that surface. Indeed one of the first successes of the STM was the imaging of the Si(111) (7×7) (Ref. 1) surface, which led to the final determination of the atomic structure of that surface.² It has also proved possible to image close packed metal surfaces,³ with atomic resolution, despite the fact that the electron states are much more delocalized. The STM can also be operated as a spectroscopic tool.⁴ With scanning tunneling spectroscopy (STS), it is possible to probe the electronic structure at different points on the surface. This is not just confined to locating surface states but also, for example, the investigation of surface adsorption⁵ and the study of chemical interactions occurring on the surface.⁶

The interpretation of STM images is not always straightforward. Difficulties could arise, for example, where electronic effects dominate over structural effects. This is exactly what happens in the case of the graphite surface, where the STM images have displayed very large corrugations.⁷ Theoretical calculations have demonstrated that this occurs because the Fermi surface has collapsed to a point at the corner of the surface Brillouin zone.⁸ Another anomaly is the Si(001) surface. STM images clearly show this surface to have a (2×1) reconstruction of symmetric dimers⁹ contrary to what is predicted by other experimental techniques¹⁰ and first principles calculations,¹¹ which suggest that the surface has in fact a $c(4\times 2)$ reconstruction of buckled dimers. It has been suggested that either the dimer is constantly flipping and the STM images the average dimer position¹² or that the tip of the STM actually causes the dimer to flip as it moves over the surface.¹³ Kageshima and Tsukada¹⁴ attempted to clarify this point by calculating STS spectra for these two reconstructions. Their calculated spectrum for the (2×1) reconstruction did not match the experimental spectrum⁹ for the surface that imaged as a (2×1) reconstruction, whereas their spectrum for the $c(4\times 2)$ reconstruction did. This provides extra evidence that although the experimental im-

age appears to be the (2×1) reconstruction, the surface may well, in fact, be the $c(4\times 2)$ reconstruction. This example illustrates that theoretical calculations are of use in interpreting experimental STM images, not just by the simulation of images, but also through the simulation of STS spectra.

In this paper, we concern ourselves with the GaAs(110) surface. Previously we have examined the GaAs(001) surface.¹⁵ Our principle findings then were the following: (1) To image the positions of the As (Ga) atoms it is necessary to use a negative (positive) tip-surface bias voltage; (2) At low bias voltages STM images may not show the positions of all of the surface atoms or dimers; (3) The features of the STM images do not always correspond to the surface charge density within the given energy range, with respect to the Fermi level. We shall investigate to what extent these findings apply to the GaAs(110) surface, while comparing our simulated images with the experimental results of Feenstra *et al.*¹⁶ and discussing the subject of the buckling of the surface bond. Recently, in another paper, Feenstra¹⁷ has presented high quality spectroscopic data for the (110) surfaces of GaAs, InP, GaSb, InAs, and InSb and we look to see if our calculations can reproduce any of the features reported for GaAs.

Our chosen method for calculating STM images and STS spectra is based on the Bardeen transfer Hamiltonian approximation (BTHA).¹⁸ This approach requires nothing more for input other than the wave functions of the surface and the wave functions of the tip that we have generated using state of the art *ab initio* pseudopotential calculations.¹⁹ For the GaAs(110) surface, we take a unit cell consisting of five layers of Ga and As atoms and five layers of vacuum. A ball and stick plan view model of this surface is shown in Fig. 1. In each layer, there are four Ga and four As atoms such that the surface unit cell is four times the size of the primitive surface unit cell. This is done to ensure that the wave functions for the tip, which consists of a cluster of four Al atoms, are fully decoupled between adjacent unit cells. When the surface atoms were allowed to relax, it was found that the top layer As atoms move up out of the surface plane

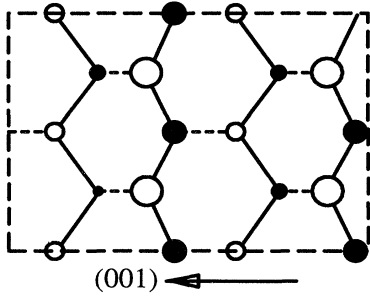


FIG. 1. Ball and stick plan view model of the GaAs(110) surface. Open (closed) circles indicate the positions of the As (Ga) atoms. Large (small) circles indicate the top (second) layer atoms.

by 0.101 Å and that the top layer Ga atoms move down by 0.510 Å. Furthermore, the As and the Ga atoms both move in the (001) direction by 0.145 Å and 0.399 Å respectively. There is also some slight relaxation of the second layer atoms. We calculate the buckling angle of the surface bond to be 27.8° in almost exact agreement with the value obtained from experiment²⁰ and other calculations.²¹ The calculated wave functions are then used to form Bardeen matrix elements,

$$M_{\mu\nu}(\mathbf{R}) = \int \psi_{\mu}^*(\mathbf{r})(H - E_{\nu})\psi_{\nu}(\mathbf{r} - \mathbf{R})d\mathbf{r},$$

where $\psi_{\mu}(\mathbf{r})$ and $\psi_{\nu}(\mathbf{r})$ are the surface and tip wave functions, respectively, and \mathbf{R} is the position of the tip relative to the surface. The tunneling current is then given by

$$I(\mathbf{R}, V_b) = \frac{2\pi e}{\hbar} \sum_{\mu\nu} |M_{\mu\nu}(\mathbf{R})|^2 [f(E_{\mu}) - f(E_{\nu})]\delta(E_{\mu} - E_{\nu} + eV_b),$$

where V_b is the tip-surface bias voltage and $f(E)$ is the Fermi distribution function. In our simulations a Gaussian function is used instead of a δ function to enable the discrete energy levels of the tip cluster to act as a continuum of levels. The main advantages of using the BTHA are that the atomic structure and wave functions are considered implicitly and that a semirealistic model of the tip may be utilized. A disadvantage of this method, however, is that because it is based on perturbation theory, it is not suitable for small tip-surface separations where there is considerable interaction between the surface and tip wave functions. Furthermore, the incomplete plane wave basis set used in the pseudopotential calculations means that the tails of the wave functions are poorly described and not suitable for use at large tip-surface separations. In our calculations, we have used throughout a constant tip-surface separation of 2 Å, which conveniently falls between these two limits. Although this is much smaller than the tip-surface separations used in the experiments, test calculations revealed that larger separations produce nearly identical images. Moreover, simulated STM images generated at constant tunneling current in which the tip moves out to larger separations also produce im-

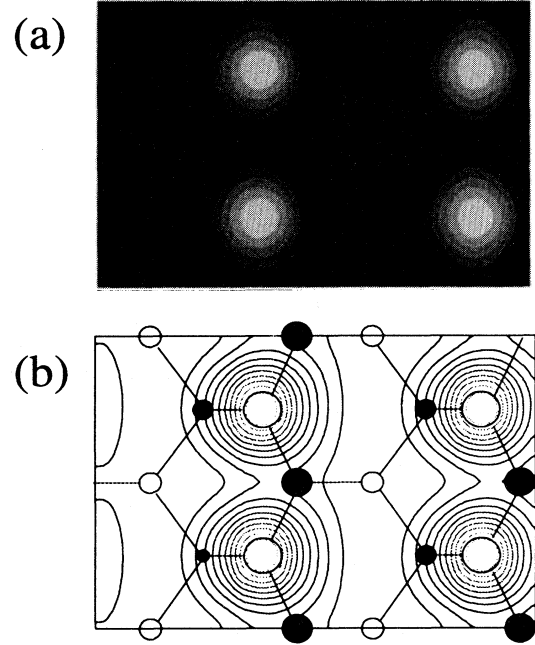


FIG. 2. (a) Simulated STM image for the GaAs(110) surface, showing the tunneling current at a constant tip-surface separation and for a bias voltage of -2 V. (b) A plot of $\int_{E_f-2\text{ eV}}^{E_f} \rho(\mathbf{r}, E)dE$ in a plane 2 Å above the surface.

ages with features in the same positions.

In Fig. 2(a), we display the simulated STM image of the tunneling current, for the GaAs(110) surface, at a constant tip-surface separation and for a bias voltage of 2 V. In our previous paper, we took the natural logarithm of the tunneling current to obtain the same effect as if the images were generated at constant tunneling current and variable tip-surface separation. Although this has the positive effect of allowing extra detail to be observed in the images, the downside is a lessening of the resolution of the images. The image in Fig. 2(a) shows pronounced bright spots corresponding exactly to the positions of the top layer As atoms. This is as expected because at a negative (positive) bias voltage the occupied (unoccupied) surface states are concentrated on the As (Ga) surface atoms. Changing the bias voltage, while still imaging occupied states, was found to have no effect on the general features of the simulated image or the positions of the bright spots. Furthermore, a plot of $\int_{E_f-2\text{ eV}}^{E_f} \rho(\mathbf{r}, E)dE$ in a plane 2 Å above the surface [Fig. 3(b)] shows that the surface charge density within this energy range corresponds exactly to the simulated STM image. This is still the case if the lower limit of the integration is altered.

Our results for positive tip-surface bias voltages are presented in Figs. 3(a)–3(c). In these simulated STM images we see that the bright spots correspond closely, but not exactly, to the positions of the Ga atoms. In fact, the bright spots are displaced in the (00 $\bar{1}$) direction, i.e., in the opposite direction to which the Ga atoms have relaxed. As the bias voltage is increased from 1 V to 3 V,

the amount of displacement diminishes. The simulated image for a bias voltage of 2 V is anomalous in that it exhibits secondary bright spots, which do not correspond to any of the atoms or bonds on the GaAs(110) surface. A plot of $\int_{E_f}^{E_f+2 \text{ eV}} \rho(\mathbf{r}, E) dE$ in a plane 2 Å above the

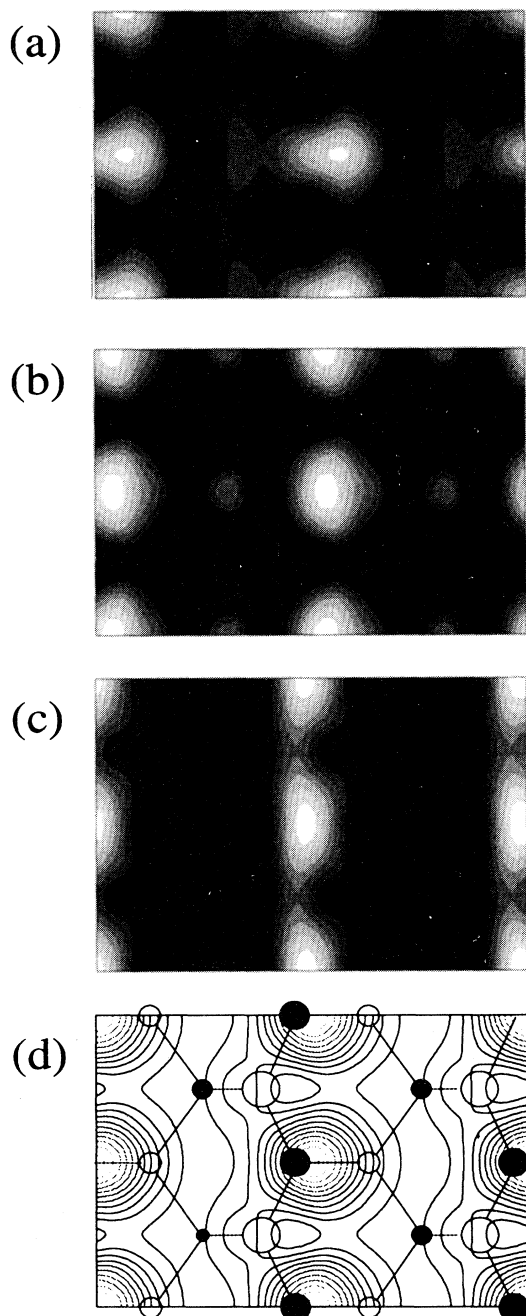


FIG. 3. (a) Simulated STM image for the GaAs(110) surface, showing the tunneling current at a constant tip-surface separation and for a bias voltage of 1 V. (b) The same as (a), but for a bias voltage of 2 V. (c) The same as (a), but for a bias voltage of 3 V. (d) A plot of $\int_{E_f}^{E_f+2 \text{ eV}} \rho(\mathbf{r}, E) dE$ in a plane 2 Å above the surface.

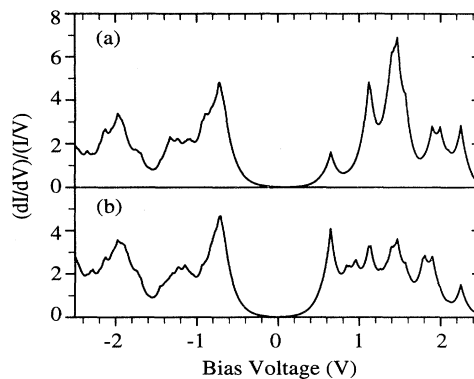


FIG. 4. (a) Simulated STS spectrum for the GaAs(110) surface with the tip positioned 2 Å directly above an As atom. (b) The same as (a), but with the tip 2 Å above a Ga atom.

surface [Fig. 3(d)] shows that the surface charge density within this energy range has features that are also displaced in the (00 $\bar{1}$) direction relative to the Ga atoms. However, the displacement of these features is less than the displacement of the bright spots in the STM images for bias voltages of 1 V and 2 V and also these features do not move if the upper limit of the integration is altered.

Feenstra *et al.*¹⁶ measured the separation, in the (001) direction, of the features corresponding to the As atoms in their experimental STM image for a negative bias voltage and the features corresponding to the Ga atoms in their images for a positive bias voltage. They also observed that the separation of the occupied and the unoccupied states obtained from theoretical calculations varied with the buckling of the surface bond. They were thus able, by comparing experiment and theory, to deduce that the buckling angle lies in the range 29°–31°. However, what our results indicate is that the STM images exaggerate the separation of the occupied and unoccupied states. Thus, the values measured by Feenstra *et al.*, from their STM images, overestimate the actual separation of the occupied and unoccupied states and thus overestimate the buckling angle. It should be pointed out that our theoretical results differ to the experimental results of Feenstra *et al.* in that they did not find the measured separations to be dependent on the bias voltage. However, they only considered a narrow range of bias voltages (0.5–1.5 V), so that any dependency on the bias voltage may not have been noticed.

In Figs. 4(a) and 4(b), we present simulated STS spectra for the GaAs(110) surface with the tip positioned 2 Å directly above an As atom and 2 Å above a Ga atom, respectively. These spectra both display a distinct band gap, which is less than the experimental value of 1.42 eV.²² This is just the usual underestimate in the band gap, due to the use of density functional theory in the calculations.²³ The Fermi level has been taken arbitrarily as the midpoint of the band gap. We observe that, although the positioning of the tip does not effect the location of the peaks in the spectra, the intensity of the peaks is dependent on the tip position. The experimental STS spectra, recently obtained by Feenstra,¹⁷ for the

GaAs(110) surface indicate that there are distinct peaks in the conduction band at energies of 0.38 eV, 0.98 eV, and 1.55 eV, relative to the conduction band edge, associated with cation derived surface states features. In our simulated spectra, there are peaks in the conduction band that can be identified with the peaks in the experimental spectra. Feenstra was not able to identify the onset of the *L*-valley bulk conduction band for GaAs. He attributed this to the close proximity of the first surface state feature obscuring the onset. This also applies to our simulated spectra. Feenstra also reported that the intensity of the peaks, but not the positions, varied with the location (and nature) of the tip in agreement with

our calculations.

In summary we have generated, using theoretical methods, STM images and STS spectra of the GaAs(110) surface. Our results demonstrate that STM images do not always correspond exactly with a plot of surface charge density within the given energy range with respect to the Fermi level. This is because the symmetries of the surface and tip wave functions are crucial in contributing to the tunneling current. One should, therefore, be careful not only when interpreting STM images, but also when taking measurements from them. Finally, we have demonstrated that our method can be used to generate STS spectra, which give good agreement with experiment.

-
- ¹ G. Binnig, H. Rohrer, Ch. Gerber, and E. Weibel, *Phys. Rev. Lett.* **50**, 120 (1983).
- ² Kunio Takayanagi, Yasumasa Tanishiro, Shigeki Takahashi, and Masaetsu Takahashi, *Surf. Sci.* **164**, 367 (1985).
- ³ V. M. Hallmark, S. Chiang, J. F. Rabolt, J. D. Swalen, and R. J. Wilson, *Phys. Rev. Lett.* **59**, 2879 (1987); J. Winterlin, J. Wiechers, H. Brune, T. Gritsch, H. Höfer, and R. J. Behm, *ibid.* **62**, 59 (1989).
- ⁴ R. M. Feenstra, *Surf. Sci.* **299/300**, 964 (1994).
- ⁵ I. Stensgaard, L. Ruan, F. Besenbacher, F. Jensen, and E. Laegsgaard, *Surf. Sci.* **269/270**, 81 (1992).
- ⁶ Qian Zhong, J. M. Vohs, and D. A. Bonnel, *Surf. Sci.* **274**, 35 (1992).
- ⁷ G. Binnig, H. Fuchs, Ch. Gerber, H. Rohrer, E. Stoll, and E. Tosatti, *Europhys. Lett.* **1**, 31 (1986); Sang-II Park and C. F. Quate, *Appl. Phys. Lett.* **48**, 112 (1986).
- ⁸ J. Tersoff, *Phys. Rev. Lett.* **57**, 440 (1986).
- ⁹ R. J. Hamers, R. M. Tromp, and J. E. Demuth, *Phys. Rev. B* **34**, 5343 (1986).
- ¹⁰ Takeshi Tabata, Tetsuya Aruga, and Yoshitada Murata, *Surf. Sci.* **179**, L63 (1987); T. Enta, S. Suzuki, and S. Kono, *Phys. Rev. Lett.* **65**, 2704 (1990).
- ¹¹ D. J. Chadi, *Phys. Rev. Lett.* **43**, 43 (1979); Zizhong Zhu, Nobuyuki Shima, and Masaru Tsukada, *Phys. Rev. B* **40**, 11 868 (1989).
- ¹² J. Ihm, D. H. Lee, J. D. Joannopoulos, and J. J. Xiong, *Phys. Rev. Lett.* **51**, 1872 (1983); Jaroslav Dabrowski and Matthias Scheffler, *Appl. Surf. Sci.* **56-58**, 15 (1992).
- ¹³ K. Cho and J. D. Joannopoulos, *Phys. Rev. Lett.* **71**, 1387 (1993).
- ¹⁴ H. Kageshima and M. Tsukada, *Phys. Rev. B* **46**, 6928 (1992).
- ¹⁵ J. M. Bass and C. C. Matthai, *Phys. Rev. B* **50**, 11 212 (1994); J. M. Bass, C. C. Matthai, and K. A. Saynor, in *Proceedings of the 22nd International Conference on the Physics of Semiconductors, 1994*, edited by David J. Lockwood (World Scientific, Singapore, 1995), p. 419.
- ¹⁶ R. M. Feenstra, Joseph A. Stroscio, J. Tersoff, and A. P. Fein, *Phys. Rev. Lett.* **58**, 1192 (1987).
- ¹⁷ R. M. Feenstra, *Phys. Rev. B* **50**, 4561 (1994).
- ¹⁸ J. Bardeen, *Phys. Rev. Lett.* **6**, 57 (1961); Masaru Tsukada, Katsuyoshi Kobayashi, Nobuyuki Isshiki, and Hiroyuki Kageshima, *Surf. Sci. Rep.* **13**, 265 (1991).
- ¹⁹ M. C. Payne, M. P. Teter, D. C. Allan, T. A. Arias, and J. D. Joannopoulos, *Rev. Mod. Phys.* **64**, 1045 (1992).
- ²⁰ S. Y. Tong, A. R. Lubinsky, B. I. Mrstik, and M. A. Van Hove, *Phys. Rev. B* **17**, 3303 (1978).
- ²¹ D. J. Chadi, *Phys. Rev. Lett.* **41**, 1062 (1978); K. C. Padney, *ibid.* **49**, 223 (1982).
- ²² J. S. Blakemore, *J. Appl. Phys.* **53**, R123 (1982).
- ²³ R. W. Godby, M. Schlüter, and L. J. Sham, *Phys. Rev. B* **37**, 10 159 (1988).

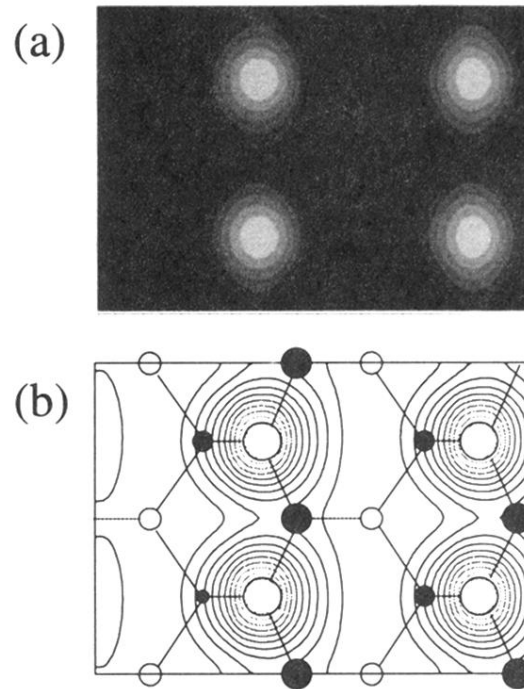


FIG. 2. (a) Simulated STM image for the GaAs(110) surface, showing the tunneling current at a constant tip-surface separation and for a bias voltage of -2 V. (b) A plot of $\int_{E_f-2 eV}^{E_f} \rho(\mathbf{r}, E) dE$ in a plane 2 \AA above the surface.

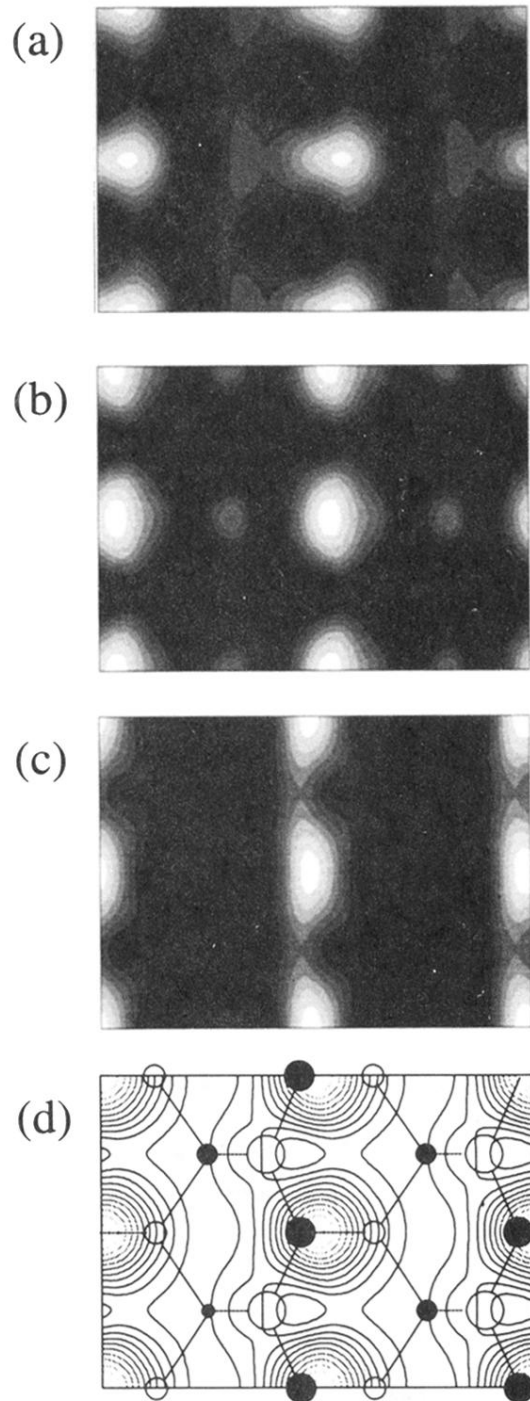


FIG. 3. (a) Simulated STM image for the GaAs(110) surface, showing the tunneling current at a constant tip-surface separation and for a bias voltage of 1 V. (b) The same as (a), but for a bias voltage of 2 V. (c) The same as (a), but for a bias voltage of 3 V. (d) A plot of $\int_{E_f}^{E_f+2 \text{ eV}} \rho(\mathbf{r}, E) dE$ in a plane 2 Å above the surface.